An official publication of the International Society for Energy, Environment and Sustainability (ISEES)

Journal of Energy and Environmental Sustainability

Journal homepage:www.jees.in

Startup of Microbial Fuel Cells with Pure Ferric Iron-reducing Bacteria Isolates

Lihong Liu[1,2], Duu-Jong Lee[3,4,*], Aijie Wang[2], Nanqi Ren[2], Lei Zhang[1], Jia-Nian Shen[1]

[1]*School of Earth Sciences, Northeast Petroleum University, Daqing 163318, China*
[2]*State Key Laboratory of Urban Water Resource and Environment, Harbin Institute of Technology, Harbin 150090, China*
[3]*Department of Chemical Engineering, National Taiwan University of Science and Technology, Taipei 106, Taiwan*
[4]*Department of Chemical Engineering, National Taiwan University, Taipei 106, Taiwan*

ARTICLE INFO

Received : 30 July 2015
Revised : 13 September 2015
Accepted : 23 September 2015

Keywords:
Microbial fuel cell
Iron-reducing bacteria
Gram - positive
Gram-negative

ABSTRACT

Ferric iron-reducing bacteria (FRB) can transfer intercellular electrons to a surrounding solid, a function also exhibited by the anode-respiring bacteria for microbial fuel cells (MFC). This study isolated from river sediment two FRB, a Gram-negative strain (*Geobaccter* sp. LAR-2, GenBank No. KC211015) and a Gram-positive strain (*Clostridium* sp. LAR-3, GenBank No. KC211016), and individually started up MFC using these two isolates as inocula at anodic compartment. The LAR-2-MFC had an open-circuit voltage (OCV) of 610 mV and maximum power density (P_{max}) of 860 mW m^{-2}. The corresponding OCV and P_{max} of LAR-3-MFC were 630 mV and 310 mW m^{-2}, respectively. The resistances of electron transfer across anodic biofilms, eletrolytes and cathodes were characterized. The tests with these two FRB support the hypothesis with FRB being effectively functioned as anode-respiring bacteria for MFC.
Keywords: Microbial fuel cell; Iron-reducing bacteria; Gram-positive; Gram-negative

1. Introduction

The microbial fuel cells (MFCs) can oxidize electron donors on anode and transfer the excess electrons through external loading to cathodes to be received by electron acceptors [Inoue et al., 2013; Chou et al., 2014; Yoshizawa et al., 2014; Zhang et al., 2015; Koroglu et al., 2014]. For instance, when sulfide and oxygen are used respectively as the electron donor and acceptor, a sulfide-MFC can be established [Lee et al., 2012].

The bioactivity of anode-respiring bacteria (ARB) in anodic biofilm often determines the performance of an MFC [Mohan et al., 2014]. The ARB can conduct extracellular electron transfer via direct electron transfer (DET) and/or mediated electron transfer (MET) [Kim et al. 1999], which is also held by iron-reducing bacteria (FRB), such as *Shewanella* and *Geobacter* sp., that can grow upon reduction of Fe(III) [Kostka et al. 2002]. Most ARB strains were identified from anodic biofilm of an operating MFC (recent review is available in [Huang et al., 2015]. Conversely, the studies on the use of pure cultures FRB isolated from non-MFC samples as inoculum for startup of an MFC are rare [Liu et al., 2014].

The confirmation of the capability of an FRB to function as an ARB has practical significance for rapid screening effective exoelectrogenic bacteria for MFC handling very different substrates. However, it is unclear whether both Gram-positive and Gram-negative FRB isolated from the same environmental site can be effective to start up an MFC. Mixed culture tests encounter difficulty for detailed interpretation of experimental data. This study isolated two strains from environmental samples with high iron-reducing capability. These two strains, one is a Gram-positive bacterium and the other is a Gram-negative bacterium, were individually used as inoculum for anodic compartment of MFCs.

2. Material and Methods

2.1 Strain screening, isolation and identification

Sludge samples were collected from sediment at intersection of A-Shi River and Songhua River, Heilongjiang, China. The samples were cultivated in tubes with iron-reducing medium (per liter): ($NaHCO_3$, 2.5 g; KH_2PO_4, 0.6 g; NH_4Cl, 1.5 g; yeast extract 0.5 g; sodium acetate, 1.36 g; Ferric citrate, 50 mM; Wolfe's vitamin solution, 5 ml; Wolfe's trace metal solution, 10 ml; pH 6.9) at 30°C. The medium was shaken at 130 rpm. Those with white, black or gray precipitates were collected for identification. The sediment was then seeded to fresh iron-reducing medium for another run of cultivation. This procedure was repeated for over ten times to enrich the consortium.

The so-obtained consortium was then diluted and spread onto the solidified agar tubes containing iron-reducing medium. The colonies formed on the agar were pickup and diluted and spread on new agar. This process was repeated for more than ten times. The cell morphology of the so-obtained isolates was observed by a phase-contrast microscope. The biochemical characteristics of the isolates were highlighted using API 20A, API-20NE and API-ZYM. The fatty acids were extracted, saponified

* *Corresponding Author: E-mail: djlee@ntu.edu.tw*

and methylated according to the protocol of the Sherlock Microbial Identification System (MIDI). The genomic DNA of collected cells was extracted using the PowerSoil DNA Isolation Kit (MoBio, Carlsbad, CA, USA) following the manufacturer's instructions. The procedures of 16S rRNA gene identification by polymerase chain reaction (PCR) and denaturing gradient gel electrophoresis (DGGE) tests were available in [Zhang et al., 2015]. Purified PCR products were ligated to vector pMD19 and cloned into *Escherichia coli* DH5á competent cells. The randomly selected 50 clones were sequenced using the ABI Prism model 3730XL (Applied Biosystems, CA, USA). The 16S rRNA gene sequences were analyzed using BLASTN and EzTaxon.

2.2 MFC and tests

Two double-chambered MFCs of size 7×7 cm^2 and length 10.5 cm were started up with the isolates obtained in Sec. 2.1. A Ultrex CMI-7000 membrane (Ultrex Membrane International Inc., Glen Rock, NJ, USA) was the cation exchange membrane (CEM). Both anodes and cathodes were made of carbon cloth of area 14.0 cm^2 (W0S1002, CeTech. Co., Taichung, Taiwan). The cathode contained 0.5 mg/cm^2 Pt catalyst. Other reactor details are available in [Liu et al., 2011].

Before MFC tests, the anode compartment was degassed. Both electrodes were hung from titanium wires and were connected through an external 1000Ù resistor. Reference Ag/AgCl electrode (type 217, XianRen Industries Co., Shanghai, China) was installed into the anodic chamber for conducting electrochemical measurements.

The enriched Fe(III)-reducing consortium was fed into the anode chamber of the MFC for cultivation in medium (per liter): Na_2HPO_4 4.57 g, NaH_2PO_4 2.45 g, NH_4Cl 0.31 g, Wolfe's vitamin solution 5 ml, and Wolfe's mineral solution 12.5 ml, pH 6.9. NaAc (20 mM) was used as carbon source for all MFC tests. The cathodic medium was a mixture of 50 mM potassium ferricyanide and 100 mM PBS.

The voltage drop over an external load 1000Ω of individual MFC was recorded at 180 s intervals. Linear sweep voltammetry (LSV) of tested MFC were conducted at 1 mV/s [Nien et al., 2011; Watson et al. 2011] using an electrochemical workstation (model CHI611, CH Instruments, Inc. Austin, TX, USA). The CV tests were conducted on anode from -0.6 to +1.0 V. The electrochemical impedance spectroscopy (EIS) experiments were performed by Zahner™ IM6ex potentiostat-AC frequency analyzer equipment with frequency of the AC signal was varied from 100 kHz to 10 mHz with an amplitude of 5 mV. Impedance experiments were performed under galvanostatic closed circuit conditions at 400 mA for the tested biofilms. The initial electrical potentials for anode tests and for cathode tests were at -0.5 V and +0.25 V, respectively.

2.3 Other measurements

The XRD spectra of dried samples were obtained with a Bruker D8 Advance X-ray Diffractometer (Bruker AXS, Congleton, UK) with a Cu anode (40 kV and 30 mA) and canning from 5° to 90°. Cell lipids were extracted with the modified as described by [Santala et al., 2011] and were characterized by direct trans-esterification-gas chromatography method with methyl pentadeconate as an internal standard.

3. Results and Discussion

3.1 Strain isolation and identification

Two isolates, LAR-2 and LAR-3, obtained from the screening and cultivation process showed efficient Fe(III)-reducing capability (suspension colors in cultivation tubes as indicators). The XRD patterns (not shown) for the freeze-dry precipitates from these suspension showed characteristic peaks for $FeCO_3$. Hence, the isolates have convert Fe(III) into Fe(II) during Fe(III)-reducing tests.

Atomic force microscope observation (not shown) reveals that the strain LAR-2 is short rod-shaped, no capsule-forming, with flagellum, 0.5–0.7 ¼m wide and 0.8–1 ¼m long microorganism. Also, the strain LAR-3 is short rod-shaped, no capsule, with flagellum, 0.3–0.5 ìm wide and 0.8–1 ìm long microorganism.

The physiological analysis (Tables 1 and 2) shows that both LAR-2 and LAR-3 can utilize urea, glucose, mannitol, lactose, sucrose, maltose, salicin, xylose, cattle gelatin, esculin, citrate, glycerol, mannose, melezitose, raffinose, sorbitol and trehalose, but cannot utilize cellobiose or rhamnose. The differences are the former cannot use tryptophan and arabinose while the latter can. Both strains contain alkaline phosphatase, esterase (C4), esterase (C8), leucine arylamidase, cystine arylamidase, trypsin, chymotrypsin, acid phosphatase, naphtha-AS-BI-phosphohydrolase, a-galactosidase, â-galactosidase, a-glucosidase, â-glucosidase, but do not have esterase (C14), leucine aromatic aminotransferase, â-glucuronidase, a-nannosidase, â-fucosidase. LAR-2 has N-acetyl-glucosaminidase but has no leucine aromatic aminotransferase; LAR-3 has valine arylamidase.

The FAME chromatograms (Tables 3 and 4) revealed the major peaks with predominant fatty acids. Comparison with database reveal no fitting based on FAME spectra for either LAS-2 or LAR-3.

The 16S rRNA sequence analysis revealed that strain LAR-2 belongs to delta subclass of the Proteobacteria and most closely related to *Geobacter sulfurreducens* PCA$^{(T)}$ (98.41%), *Geobacter hydrogenophilus* H2$^{(T)}$(95.11%) (Table 5). The phylogenetic analyses based on 16S rRNA gene sequences indicated that the strain LAR-2 formed a lineage in the Deltaproteobacteria (Fig. 1a). Meanwhile, the 16S rRNA sequence analysis revealed that strain the LAR-3 belongs to Clostridia and most closely related

Table 1. Physiological and biochemical tests for isolates*

API-A			API-20NE		
Carbon source	LAR-2	LAR-3	Substrate	LAR-2	LAR-3
IND	-	+	NO3	+	+
URE	+	+	TRP	+	+
GLU	+	+	GLU	+	+
MAN	+	+	ADH	+	-
LAC	+	+	URE	+	+
SAC	+	+	ESC	+	+
MAL	+	+	GEL	+	+
SAL	+	+	PNPG	+	+
XYL	+	+	GLU	+	+
ARA	-	+	ARA	+	+
GEL	+	+	MNE	+	+
ESC	+	+	MAN	+	+
GLY	+	+	NAG	+	+
CEL	+	+	MAL	+	+
MNE	+	+	GNT	+	+
MLZ	+	+	CAP	-	-
RAF	+	+	ADI	-	-
SOR	+	+	MLT	+	+
RHA	-	+	CIT	+	+
TRE	+	+	PAC	+	+
SPOR	-	+			
GRAM	pink	purple			
COCC	rod	rod			

*Includes urea, glucose, mannitol, lactose, sucrose, maltose, salicin, xylose, cattle gelatin, esculin, ferric citrate, glycerol, mannose,melezitose, raffinose, sorbitol, trehalose, tryptophan, arabinose, cellobiose andrhamnose.

Table 2. Physiological API-ZYM identification for isolates.

Enzyme	LAR-2	LAR-3
control	-	-
alkaline phosphatase	+	+
esterase (C4)	+	+
esterase lipase (C8)	+	+
esterase (C14)	-	-
leucine arylamidase	+	+
valine arylamidase	+	+
cysteineacrylamidase	+	+
trypsin	+	+
chymotrypsin	+	+
acid phosphatase	+	+
naphtha-AS-BI-phosphohydrolase	+	+
a-galactosidase	+	+
â-galactosidase	+	+
â-glucuronidase	-	-
a-glucosidase	+	+
â-gucosidase	+	+
N-acylglucosaminidase	+	-
a-nannosidase	-	-
â-fucosidase	-	-

Table 3. Identification of fatty acids of LAR-2.

No.	RT	Response	Peak Name	Percent	Comment1
1	3.162	857	10:00	0.34	
2	4.779	655	12:00	0.25	
3	6.932	419	14:0 anteiso	0.15	
4	10.215	20408	Sum In Feature 3	7.19	16:1 w7c/16:1 w6c
5	10.519	119599	16:00	42.03	
6	12.261	527	17:00	0.18	
7	13.522	1811	Sum In Feature 5	0.62	18:2 w6,9c/18:0 ante
8	13.619	54712	18:1 w9c	18.79	
9	13.713	37567	Sum In Feature 8	12.89	18:1 w7c
10	14.021	5384	18:00	1.84	
11	15.11	8543	19:0 iso	2.91	
12	15.608	37656	19:0 cyclo w8c	12.79	0

Table 4. Identification of fatty acids of LAR-3.

No.	RT	Response	Peak Name	Percent	Comment
1	3.145	599	10:00	0.21	
2	4.761	642	12:00	0.21	
3	7.287	26210	14:00	8.21	
4	10.196	26508	Sum In Feature 3	8.02	16:1 w7c/16:1 w6c
5	10.501	136208	16:00	41.07	
6	12.042	2556	17:0 cyclo	0.76	
7	12.235	381	17:00	0.11	
8	13.501	1355	Sum In Feature 5	0.4	18:2 w6,9c/18:0 ante
9	13.593	28705	18:1 w9c	8.43	
10	13.689	18064	Sum In Feature 8	5.3	18:1 w7c
11	14	4238	18:00	1.24	
12	14.133	877	18:1 w7c 11-methyl	0.26	
13	14.839	1372	19:1 iso I	0.4	
14	15.089	7018	19:0 iso	2.04	
15	15.526	21043	Sum In Feature 7	6.11	19:0 cyclo w10c/19w6
16	15.586	58579	19:0 cyclo w8c	17	
17	17.037	771	20:2 w6,9c	0.22	

Table 5. Blast results of strain LAR-2 based on the 16S rRNA genes.

Name	Accession No	Similarity(%)	Diff/Total nt
Geobacter sulfurreducens PCA$^{(T)}$	AE017180	98.41	24/1514
Geobacter hydrogenophilus H2$^{(T)}$	U28173	95.11	68/1391
Geobacter metallireducens GS-15$^{(T)}$	CP000148	94.78	79/1514
Geobacter grbiciae TACP-2$^{(T)}$	AF335182	94.66	80/1499
Geobacter pickeringii G13$^{(T)}$	DQ145535	94.41	84/1504
Geobacter argillaceus G12$^{(T)}$	DQ145534	93.5	95/1461
Geobacter pelophilus Dfr2$^{(T)}$	U96918	92.87	105/1473
Geobacter thiogenes JCM 14045$^{(T)}$	AF223382	92.8	109/1513
Geobacter lovleyi SZ$^{(T)}$	CP001089	92.6	112/1513
Geobacter luticola OSK6$^{(T)}$	AB682759	92.55	110/1476
Geobacter bemidjiensis Bem$^{(T)}$	CP001124	92.46	114/1511
Geobacter chapellei 172$^{(T)}$	U41561	92.41	111/1463
Geobacter daltonii FRC-32$^{(T)}$	CP001390	92.33	116/1512
Geobacter uraniireducens Rf4$^{(T)}$	CP000698	92.26	117/1512
Geobacter psychrophilus P35$^{(T)}$	AY653549	92.18	116/1484
Geobacter bremensis Dfr1$^{(T)}$	U96917	92.12	116/1472
Geobacter toluenoxydans TMJ1$^{(T)}$	EU711072	92	115/1438
*Syntrophus buswellii*DSM 02612$^{(T)}$	X85131	85.92	213/1513
Geobacter sulfurreducens PCA$^{(T)}$	AE017180	98.41	24/1514
Geobacter hydrogenophilus H2$^{(T)}$	U28173	95.11	68/1391
Geobacter metallireducens GS-15$^{(T)}$	CP000148	94.78	79/1514
Geobacter grbiciae TACP-2$^{(T)}$	AF335182	94.66	80/1499
Geobacter pickeringii G13$^{(T)}$	DQ145535	94.41	84/1504
Geobacter argillaceus G12$^{(T)}$	DQ145534	93.5	95/1461
Geobacter pelophilus Dfr2$^{(T)}$	U96918	92.87	105/1473
Geobacter thiogenes JCM 14045$^{(T)}$	AF223382	92.8	109/1513
Geobacter lovleyi SZ$^{(T)}$	CP001089	92.6	112/1513
Geobacter luticola OSK6$^{(T)}$	AB682759	92.55	110/1476
Geobacter bemidjiensis Bem$^{(T)}$	CP001124	92.46	114/1511
Geobacter chapellei 172$^{(T)}$	U41561	92.41	111/1463
Geobacter daltonii FRC-32$^{(T)}$	CP001390	92.33	116/1512
Geobacter uraniireducens Rf4$^{(T)}$	CP000698	92.26	117/1512
Geobacter psychrophilus P35$^{(T)}$	AY653549	92.18	116/1484

to *Clostridium celerecrescens* DSM 5628$^{(T)}$(99.45%), *Clostridium sphenoides* DSM 632$^{(T)}$(98.83%), *Clostridium indolis* DSM 755$^{(T)}$(98.28%), *Clostridium methoxybenzovorans* SR3$^{(T)}$(98.23%), *Clostridium saccharolyticum* WM1$^{(T)}$(98.02%) (Table 6). The phylogenetic analyses based on 16S rRNA gene sequences indicated that the strain LAR-3 formed a lineage in the Clostridiales (Fig. 1b).

On the basis of the above characterization, the strain LAR-2 is a Gram-negative, no spore-forming, and anaerobic bacterium, confirmed to be closely affiliated to *Geobacter* sp.. The gene sequence was deposited in GenBank under accession no. KC211015. The strain LAR-3 is a Gram-positive, spore-forming and anaerobic bacterium, confirmed to be closely affiliated to *Clostridium* sp. with gene sequence accession number at GenBank No. KC211016.

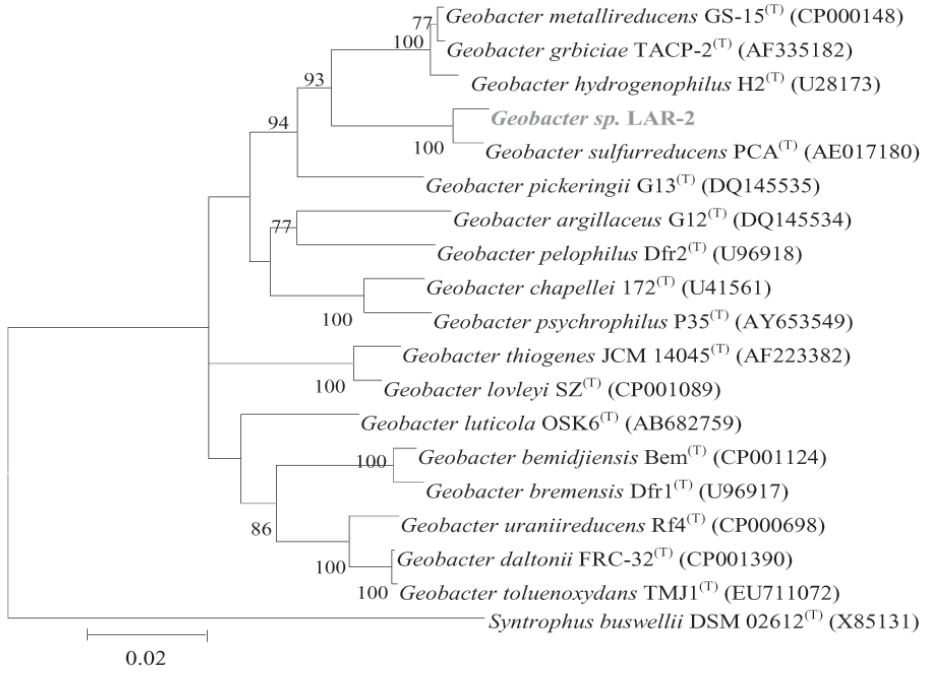

(a)

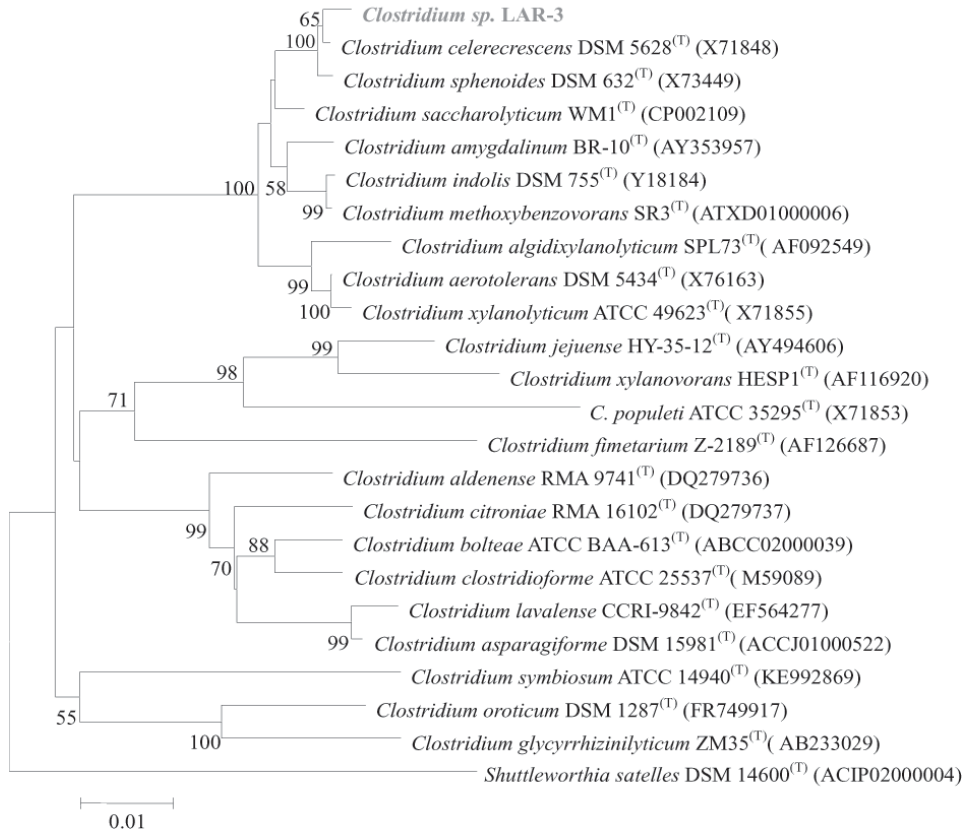

Fig. 1. Neighbor-joining showing phylogenetic positions of isolated strains LAR-2(a) /LAR-3 (b)and related species based on 16S rRNA gene sequence comparisons. Bootstrap values are indicated at nodes. Only bootstrap values >50% are shown. Scale bar, 1% sequence dissimilarity (one substitution per 100 nt). Representative sequences in the dendrogram were obtained from EzTaxon (accession number in parentheses).

Table 6. Blast results of strain LAR-3 based on the 16S rRNA genes.

Name	Accession	Pairwise Similarity(%)	Diff/Total nt
Clostridium celerecrescens DSM 5628(T)	X71848	99.45	8/1462
Clostridium sphenoides DSM 632(T)	X73449	98.83	17/1457
Clostridium indolis DSM 755(T)	Y18184	98.28	25/1457
Clostridium methoxybenzovorans SR3(T)	ATXD01000006	98.23	26/1467
Clostridium saccharolyticum WM1(T)	CP002109	98.02	29/1466
Clostridium amygdalinum BR-10(T)	AY353957	97.59	35/1451
Clostridium aerotolerans DSM 5434(T)	X76163	97.55	35/1426
Clostridium xylanolyticum ATCC 49623(T)	X71855	97.12	42/1456
*Clostridium algidixylanolyticum*SPL73(T)	AF092549	96.93	45/1466
Clostridium bolteae ATCC BAA-613(T)	ABCC02000039	93.86	90/1465
Clostridium aldenense RMA 9741(T)	DQ279736	93.68	87/1376
Clostridium clostridioforme ATCC 25537(T)	M59089	93.08	101/1459
Clostridium lavalense CCRI-9842(T)	EF564277	93.04	100/1436
Clostridium symbiosum ATCC 14940(T)	KE992869	92.97	103/1466
Clostridium asparagiforme DSM 15981(T)	ACCJ01000522	92.97	103/1465
Clostridium citroniae RMA 16102(T)	DQ279737	92.82	102/1420
*Clostridium oroticum*DSM 1287(T)	FR749917	92.62	108/1463
Clostridium glycyrrhizinilyticum ZM35(T)	AB233029	92.01	117/1465
*Clostridium jejuense*HY-35-12(T)	AY494606	91.89	117/1443
Clostridium fimetarium Z-2189(T)	AF126687	91.61	123/1466
*Clostridium xylanovorans*HESP1(T)	AF116920	91.01	131/1457
*Clostridium populeti*ATCC 35295(T)	X71853	90.56	137/1451
Shuttleworthiasatelles DSM 14600(T)	ACIP02000004	89.21	158/1464

3.2 MFC tests

3.2.1 LAR-2

Figure 2a shows the *V-t* curves for LAR-2-MFC. After a lag phase of 25 d, the cell voltage was increased to about 310 mV, then fluctuated in the next 10 d. The peak voltage gradually increased to over 600 mV since 2nd cycle, indicating formation of mature anodic biofilm in MFC. The LAR-2-MFC was successfully started up.

The LAR-2-MFC had an OCV of 610 mV (Fig. 2b). Reducing external load yielded an increase in electrical current and reduction in cell voltage. The mild initial drop in voltage indicates the presence of activation losses of 5 mV. When reaching *V*=470 mV, the power density peaked at 860 mW m^{-2}. The short circuit current density (I_{sc}) was 1.67 A m^{-2}. The cell power shoot proposed by [Nien et al., 2011] was noted for the present MFC.

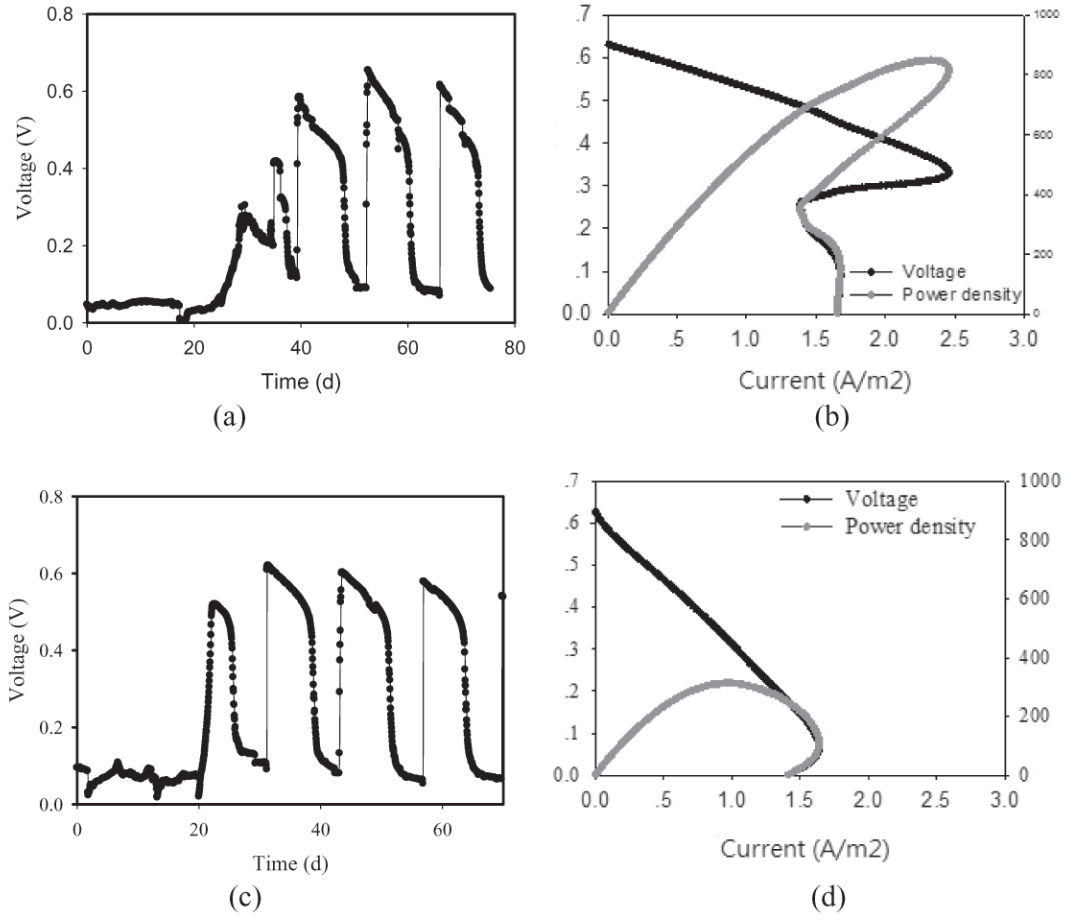

Fig. 2. MFC performance after startup. (a) V-t curve. LAR-2, voltage in mV. (b) Polarization curve and power density curve for LAR-2. Power density in mW/m^2. (c) V-t curve. LAR-3, voltage in mV. (d) Polarization curve and power density curve for LAR-3. Power density in mW/m^2.

Nyquist plots (Fig. 3a) for the LAR-2-MFC revealed a typical MFC performance curve. The electrolyte resistances were low (<10Ù). The polarization resistances for anode and cathode were estimated by the diameters for the first semi-circles as 65Ù and 70Ù, respectively. The biofilm-anode polarization resistance was estimated based on the diameter for the second semi-circle as 740Ù for anode. The anodic biofilm of LAR-2-MFC had high activity but contributed principally the cell resistance in the test.

3.2.2 LAR-3

Figure 2c shows the *V-t* curves for LAR-3-MFC. After a lag phase of 20 d, the cell voltage was increased to about 520 mV, then gradually dropped to <100 mV in next 5–8 d. The peak voltage gradually increased from 520 mV to over 600 mV since 2nd cycle, indicating successful startup of the MFC.

The LAR-3-MFC had an OCV of 630 mV (Fig. 2d) and P_{max}=323 mW m^{-2} at V=415 mV. The short circuit current density (I_{sc}) was 1.41 A m^{-2}. The cell power shoot was also observed for this MFC. Nyquist plots (Fig. 3b) estimated the polarization resistances for anode and cathode to be 610Ù and 190Ù, respectively.

3.3 FRB for MFC startup

This study confirmed that the two isolated FRB can be independently used as the inoculum for developing anodic biofilms of MFC. The so-started up MFC has high OCV, suggesting high bioelectrochemical activity of the cultivated LAR-2 and LAR-3 biofilms.

The extracellular electron transfer can be achieved by *c*-type cytochrome proteins in the outer membrane of FRB with heme being the active center or by yielding electron shutters. The electrolyte resistances for anode, cathode and whole cells ranged 10–20 Ù, suggesting low electrolyte resistance in the tested MFC cell. The *Geobacter sp.* is a Gram-negative strain that has thin cell walls. Conversely, The *Clostridium sp.* is a Gram-positive strain that has thick cell wall. The nature of cell walls may affect the observed biofilm polarization resistance for anode, 65Ù for LAR-2 and 610Ù for LAR-3. Reguera et al. [2005] proposed that their *Geobacter* strain utilized conductive pili for transferring electron to the surface of iron oxides. Park et al. [2001] proposed that their *Clostridium* strain may utilize direct electron transfer (DET) pathway in MFC operation. The more efficient electron pathway by *Geobacter* sp. may also correspond to the higher P_{max} (860 mW m^{-2}) than for the *Clostridium* sp. (313 mW m^{-2}).

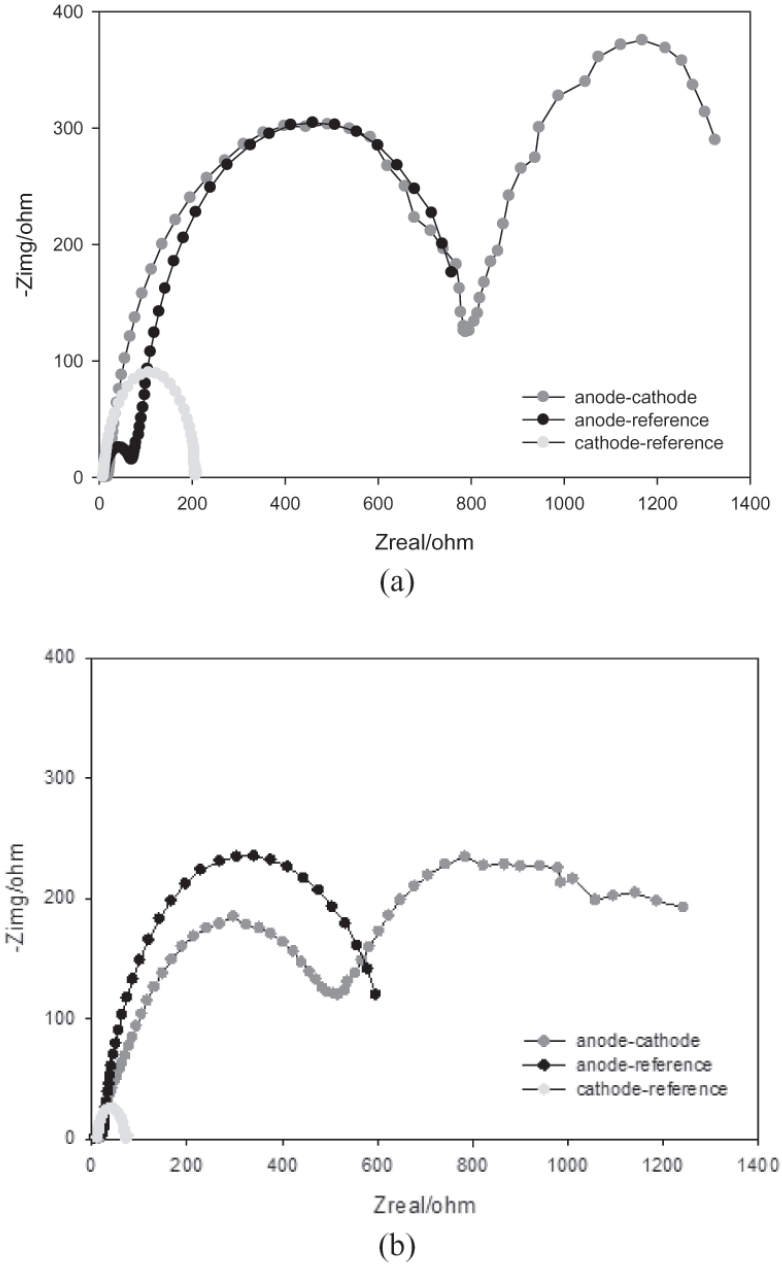

Fig. 3. Nyquist plot for anode, cathode and whole cell. (a) LAR-2-MFC, (b) LAR-3-MFC.

Power overshoot occurred in both LAR-2 and LAR-3 tests. Restated, as external loads were decreased, the cell resistance suddenly increased leading to decreases in both cell voltage and electrical current under high electrical current regimes. Power overshoot is commonly noted for MFC with mixed culture [Liu et al., 2011; Nien et al., 2011; Ieropoulos et al., 2010]. The present observations confirmed that the MFCs with single cultures can also have power overshoot. The sudden increase in resistance for extracellular electron transfer on anode surface is proposed to induce the occurrence of power overshoot [Nien et al., 2011]. The present study revealed that both Gram-positive and Gram-negative strains can have power overshoot, hence the electron saturation at cell membrane for all bacterial strains can occur at high current conditions. This is not welcome since the occurrence of power overshoot limits the cell output. Mature biofilm with excess exoelectrogens may lead to high MFC current, but the increment will not be unlimited owing to the biological nature of FRB in the biofilm

4. Conclusions

The *Geobacter* sp. LAR-2 (Gram-negative) and the *Clostridium* sp. LAR-3 (Gram-positive) were isolated and identified using biochemical tests and PCR-DGGE tests. These two strains were confirmed to be FRB via XRD tests on the precipitate yielded. The LAR-2-MFC was successfully started up with OCV of 610 mV, P_{max}=860 mW m^{-2} and polarization resistance for anode of 65Ù. The LAR-3-MFC was also started up with OCV=630 mV, P_{max}=323 mW m^{-2}, and polarization resistances for anode of 610Ù. These two FRBs were confirmed to be functioning well as ARB for MFC, with the former being a preferred FRB for MFC operation than the latter. The MFCs with single cultures can also have power overshoot

5. Acknowledgements

This work is supported by NSFC project No. 51278128.

6. References

1. Inoue K, Ito T, Kawano Y, Iguchi A, Miyshara M, Suzuki Y, Watabane K., 2013. Electricity generation from cattle manure slurry by cassette-electrode microbial fuel cells, *Journal of Bioscience and Bioengineering* 116, 610–615.
2. Chou TY, Whiteley CG, Lee DJ, 2014. Anodic potential on dual-chambered microbial fuel cell with sulphate reducing bacteria biofilm. *International Journal of Hydrogen Energy* 39, 19225–19231.
3. Yoshizawa T, Miyahara M, Kouzuma A, Watanabe K, 2014. Conversion of activated-sludge reactors to microbial fuel cells for wastewater treatment coupled to electricity generation. *Journal of Bioscience Bioengineering* 118, 533–539 (2014).
4. Zhang GD, Zhao QL, Jiao,Y, Lee DJ, 2015. Long-term operation of manure-microbial fuel cell. *Bioresource Technology* 180, 365–369.
5. Koroglu EO, Ozkaya B, Denktas C, Cakmakci M, 2014. Electricity generating capacity and performance deterioration of a microbial fuel cell fed with beer brewery wastewater. *Journal of Bioscience and Bioengineering* 118, 672–678.
6. Lee CY, Ho KL, Lee DJ, Su A, Chang JS, 2012. Electricity harvest from nitrate/sulfide-containing wastewaters using microbial fuel cell with autotrophic denitrifier, *Pseudomonas* sp. C27. *International Journal of Hydrogen Energy* 37, 15827–15832.
7. Mohan SV, Velvizhi G, Modestra JA, Srikanth S, 2014. Microbial fuel cell: Critical factors regulating bio-catalyzed electrochemical process and recent advancements. *Renewable and Sustainable Energy Reviews* 40, 779–797.
8. Kim BH, Kim HJ, Hyun MS, Park DH, 1999. Direct electrode reaction of Fe(III)-reducing bacterium, *Shewanella putrefaciens*. *Journal of Microbiology and Biotechnology* 9, 127–131.
9. Kostka JE, Dalton DD, Skelton H, Dollhopf S, Stucki JW, 2002. Growth of iron(III)-reducing bacteria on clay minerals as the sole electron acceptor and comparison of growth yields on a variety of oxidized iron forms. *Applied and Environmental Microbiology* 68, 6256–6262.
10. Huang JJ, Zhu NW, Cao YL, Peng Y, Wu PX, Dong WH, 2015. Exoelectrogenic bacterium phylogenetically related to *Citrobacter freundii*, isolated from anodic biofilm of a microbial fuel cell. *Applied Biochemistry and Biotechnology* 175, 1879–1891.
11. Liu TX, Li XM, Zhang W, Hu M, Li FB, 2014. Fe(III) oxides accelerates microbial nitrate reduction and electricity generation by *Klebsiella pneumoniae* L17. *Journal of Colloid and Interface Science* 423, 25–32.
12. Liu LH, Lee CY, Ho KC, Nien PC, Su A, Wang AJ, Ren NQ, Lee DJ 2011. Occurrence of power overshoot for two chambered MFC at nearly steady-state operation. Int. J. Hydrogen Energy 36, 13896 - 13899.
13. Santala S, Efimova E, Kivinen V, Larjo A, Aho T, Karp M, Santala V, 2011. Improved triacylglycerol production in *Acinebacter baylyi* ADP1 by metabolic engineering, *Microbiol Cell Factories* 10, 36.
14. Nien PC, Lee CY, Ho KC, Adav SS, Liu LH, Wang AJ, Ren NQ, Lee DJ, 2011. Power overshoot in two-chambered microbial fuel cell (MFC). *Bioresource Technology* 102, 4742–4746.
15. Watson VJ, Logan BE, 2011. Analysis of polarization methods for elimination of power overshoot in microbial fuel cell. *Electrochemistry Communications*13, 54–56.
16. Reguera G, McCarthy KD, Mehta T, Nicol JS, Tuominen MT, Lovley DR, 2005. Extracellular electron transfer via microbial nanowires. *Nature* 435, 1098–1101.
17. Park HS, Kim BH, Kim HS, Kim HJ, Kim GT, Kim M, Chang IS, Park YK, Chang HI, 2001. A novel electrochemically active and Fe(III)-reducing bacterium phylogenetically related to *Citrobacter butyricum* isolated from a microbial fuel cell. *Anaerobe* 7, 297–306.
18. Ieropoulos I, Winfield J, Greenman J, 2010. Effects of flow-rate inoculum and time on the internal resistance of microbial fuel cells. *Bioresource Technology* 101, 3520–3525.